

SCENEVERSE: Scaling 3D Vision-Language Learning for Grounded Scene Understanding

Baoxiong Jia* Yixin Chen* Huangyue Yu Yan Wang Xuesong Niu
Tengyu Liu Qing Li Siyuan Huang
Beijing Institute for General Artificial Intelligence (BIGAI)
<https://scene-verse.github.io>



Figure 1. **Overview of SCENEVERSE.** A million-scale 3D vision-language dataset that comprises over 68K various 3D indoor scenes and 2.5M aligned scene-language pairs in the form of **scene caption**, **object caption**, and **object referral**.

Abstract

3D vision-language grounding, which focuses on aligning language with the 3D physical environment, stands as a cornerstone in the development of embodied agents. In comparison to recent advancements in the 2D domain, grounding language in 3D scenes faces several significant challenges: (i) the inherent complexity of 3D scenes due to the diverse object configurations, their rich attributes, and intricate relationships; (ii) the scarcity of paired 3D vision-language data to support grounded learning; and (iii) the absence of a unified learning framework to distill knowledge from

grounded 3D data. In this work, we aim to address these three major challenges in 3D vision-language by examining the potential of systematically upscaling 3D vision-language learning in indoor environments. We introduce the first **million-scale** 3D vision-language dataset, SCENEVERSE, encompassing about 68K 3D indoor scenes and comprising 2.5M vision-language pairs derived from both human annotations and our scalable scene-graph-based generation approach. We demonstrate that this scaling allows for a unified pre-training framework, Grounded Pre-training for Scenes (GPS), for 3D vision-language learning. Through extensive experiments, we showcase the effectiveness of GPS by achieving state-of-the-art performance on all existing 3D visual grounding benchmarks. The vast potential of SCEN-

* indicates equal contribution.

EVERSE and GPS is unveiled through zero-shot transfer experiments in the challenging 3D vision-language tasks.

1. Introduction

The foundation of human cognitive development lies in the grounding of language within the physical world [46, 73, 97]. Recent progress in Large Language Models (LLMs) [11, 75], often referred to as “foundation models” [10], has markedly promoted the alignment between vision and language [3, 51, 66] through utilizing billion-scale vision-language datasets [71, 96]. Nonetheless, with these advancements predominantly focusing on the 2D domain, the grounded understanding of 3D physical environments remains in an incipient stage [1, 5, 16]. Recognizing the pivotal role of grounded 3D experiences in shaping human cognition [7, 8] and the delayed research development in this area, there is a compelling need to intensify the exploration into the vision-language learning challenge, specifically in the context of 3D scenes.

Seeking insights from the 2D vision-language (2D-VL) achievements, a major factor to the success was the notable scale-up of paired vision-language data [15, 45, 71]. However, applying these principles directly from 2D to 3D is fraught with challenges. Primarily, 3D data collection heavily relies on the scanning device, making it inherently much more complex and expensive than gathering 2D images. Despite steady efforts to increase the volume of 3D scene data [9, 23, 58, 87], most datasets remain limited to thousands of scenes, substantially lagging behind the scale of existing 2D datasets. This gap is further widened by the inherent complexities of 3D scenes, which feature a multitude of object instances with diverse attributes, varying arrangements, and intricate inter-object relationships. These unique aspects of 3D scenes not only make the accurate description of objects and their relations more challenging but also considerably increase the number of language descriptions required for thorough scene depiction. Consequently, this presents a significant challenge in obtaining a sufficient supply of high-quality paired scene-language data crucial for grounded scene understanding.

To confront these challenges, we propose consolidating current efforts to build up SCENEVERSE, the first **million-scale** dataset aimed at advancing 3D vision-language (3D-VL) learning for grounded scene understanding. At the scene level, we unify 3D scene data from existing datasets [9, 23, 40, 67, 78] and supplement the collection with synthetic scenes [27, 95]. This compilation represents the most extensive 3D scene data gathered to date, amounting to 68,406 scenes for grounding. Additionally, we propose an automated generation pipeline utilizing 3D scene graphs [4, 79] and LLMs to create comprehensive, high-quality scene-language pairs. This refined collection, including 190,836 human annotated pairs and totaling 2.5M

scene-language pairs, provides detailed and comprehensive portrayals of both object-level and scene-level descriptions within the 3D scene.

We thoroughly investigate the potential offered by the data scale-up in SCENEVERSE with large-scale pre-training. Specifically, we present a novel and unified pre-training framework, Grounded Pre-training for Scenes (GPS), which is designed with scene-level and object-level alignment objectives and devoid of auxiliary losses and designs. Through multi-level contrastive alignment, we observe significant performance improvements across all existing 3D visual grounding benchmarks, achieving new state-of-the-art results through a simple and effective pre-training process. Additionally, we unveil the vast possibilities offered by SCENEVERSE and GPS in 3D-VL tasks in a zero-shot transfer setting. At last, we provide a more comprehensive understanding of the data-scaling effects in SCENEVERSE through extensive ablative experiments to point out future directions.

Our main contributions can be summarized as follows:

- We introduce SCENEVERSE, the first million-scale 3D-VL dataset for grounded scene understanding. SCENEVERSE encompasses 68K 3D scenes coupled with 2.5M scene-language pairs, sourced through a combination of human annotation and automated generation methods. This represents a significant improvement in terms of data diversity and scale compared to prior datasets.
- We propose GPS, an efficient transformer-based model trained with multi-level scene-text alignment that achieves state-of-the-art results on all existing 3D-VL grounding benchmarks, benefiting from pre-training on multi-level scene-language pairs in SCENEVERSE.
- We demonstrate that with the data scale-up and model design, our pre-trained models exhibit emerging zero-shot generalization capabilities in grounded scene understanding, paralleling the successes seen in 2D-VL models.

2. Related Work

Datasets for Grounded 3D Understanding Obtaining aligned 3D-language data is an inherently difficult task. In 3D object modeling, pioneering works like ShapeNet [14] sourced 3D assets from online repositories, leading to follow-up proliferation of high-quality 3D object datasets [22, 60, 81]. Notably, recent developments include internet-scale data collection with Objaverse [25, 26], accompanied by the integration of object-level captions [83] for 3D-language alignment. Models trained on these datasets demonstrate an enhanced understanding of objects, evident in classification [52], generation [53], and captioning tasks [55].

In contrast, developing datasets for grounded 3D scene understanding is even more challenging due to the extensive requirements for scene acquisition and annotation. Existing works curate RGB-D and scanned indoor scene datasets [9, 13, 23, 58, 67, 78] initially used for benchmark-

ing classical grounding tasks like 3D object detection and segmentation [30, 42, 59, 72, 77]. These semantically labeled scenes are subsequently applied in fine-grained scene grounding tasks like object referral [1, 16, 93], captioning [17, 19, 20, 88], vision-language-navigation [38, 56, 63, 80] and reasoning [5, 37, 57]. Recent work exploits the representation of 3D scene graphs (3DSGs) [4, 69, 79], which concisely describes scenes with hierarchical structures. This representation is notably advantageous for planning [2, 68] and captioning [33], owing to its compatibility with LLMs. Nevertheless, as shown in Tab. 1, these datasets are significantly constrained in both scene and language scales, underscoring the need for scaling up fine-grained scene-language-aligned data to enhance grounded scene understanding.

Vision-Language Learning Recent years have witnessed tremendous progress in 2D vision-language learning [3, 24, 49, 51, 66, 70, 76], empowered by transformer-based pre-training models [11, 28, 62] and large-scale image-language datasets [15, 71]. A central theme across language and 2D-VL domains is the effectiveness of data scaling [43], as demonstrated by improved alignment and expanded capabilities in open-vocabulary understanding [32, 44, 47, 50] through a simplified contrastive pre-training pipeline [66].

However, in grounded scene understanding, the primary challenge for models has been the limited availability of paired 3D scene-language data, which restricts the application of insights gained from 2D-VL. Current models for 3D scene grounding [6, 18, 35, 40, 41, 54, 82, 86, 94] heavily rely on task-specific knowledge in both model and loss designs or advanced optimization strategies [98]. To bridge this gap, there has been a growing emphasis on employing pre-trained 2D-VL models for 3D-VL [34, 36, 64, 74, 83, 91, 92]. Nonetheless, these models predominantly draw on information available from 2D-VL models (*e.g.*, object attribute, affordance, *etc.*), falling short on capturing crucial information like object spatial relationships, which are only attainable through 3D data. This urges the need for a multi-level alignment between language and 3D scenes, particularly regarding 3D-specific information. Considering the nascent stage of existing 3D pre-training methods [29, 84, 98], we believe SCENEVERSE and GPS have the potential to spearhead new avenues in 3D-VL research.

3. SCENEVERSE

SCENEVERSE is the first million-scale dataset designed for grounded scene understanding. Our 3D scenes are curated from diverse existing datasets of both real and synthetic environments. Harnessing the power of 3D scene graphs and LLMs, we introduce an automated pipeline to generate comprehensive and high-quality language for both object-level and scene-level descriptions. We additionally incorporate the most extensive human-annotated object referrals to date, providing new training sources and benchmarks in this field.

Table 1. **Comparison of SCENEVERSE with existing 3DVL Datasets.** SCENEVERSE expands the data scale of prior work by an order of magnitude. Anno.: human annotations. Syn.: template or LLM generated descriptions.

Dataset	3D Data		Language		Total
	Scene	Object	Anno.	Syn.	
ScanRefer[16]			52K	-	52K
ReferIt3D[1]			42K	200K	242K
ScanQA[5]	1.5K	33K	27K	-	27K
SQA3D[57]			-	33K	33K
Multi3DRefer[93]			52K	10K	62K
Cap3D[55]	-	666K	58K	666K	724K
ScanScribe[98]	3K	56K	94K	184K	278K
SCENEVERSE	68K	1.5M	190K	2.3M	2.5M

3.1. Scene Curation

To address the scarcity of available 3D scene data, we construct SCENEVERSE by unifying 3D scene data from various existing datasets. We use real-world scene datasets, including ScanNet [23], ARKitScenes [9], HM3D [67], 3RScan [78] and MultiScan [58], alongside synthetic environments from Structured3D [95] and ProcTHOR [27]. The inclusion of these synthetic datasets is mainly motivated by their potential as scalable data sources for 3D-VL alignment. To ensure cohesion across various sources, we conduct preprocessing steps such as room segmentation, point subsampling, axis alignment, normalization, and semantic label alignment. Each scan is represented by a point cloud $P \in \mathbb{R}^{N \times 8}$, wherein each point is defined by its 3D coordinates, RGB color, instance id and semantic label. In total, we curate 68,406 3D scenes in SCENEVERSE.

3.2. 3D Scene Graph Construction

Our 3D scene graph is defined as a set of tuples $\mathcal{G} = (\mathcal{V}, \mathcal{E})$, where the nodes \mathcal{V} comprises $\mathcal{V}_1 \cup \mathcal{V}_2 \cup \dots \cup \mathcal{V}_K$, with \mathcal{V}_k representing the set of nodes at a particular hierarchical level. Each node v represents one distinct 3D object instance, parameterized by its centroid $\mathbf{p}_i \in \mathbb{R}^3$ and bounding box size of $\mathbf{b}_i = (b_x, b_y, b_z) \in \mathbb{R}^3$. The edges \mathcal{E} represent spatial relationships between nodes.

To construct the scene graph \mathcal{G} , we first instantiate the nodes with the instance annotation from the point clouds and assign object classes with their corresponding semantic labels. Following prior work [1, 79], we consider the following spatial relations.

Vertical proximity This encompasses both in-contact relationships (*e.g.*, support, inside, embed), and non-contact ones (*e.g.*, above, below).

Horizontal proximity Horizontal relationships describe the proximity relations like in front of, next to, behind, *etc.* Relationships like left, right are contextually dependent on a reference view, where another

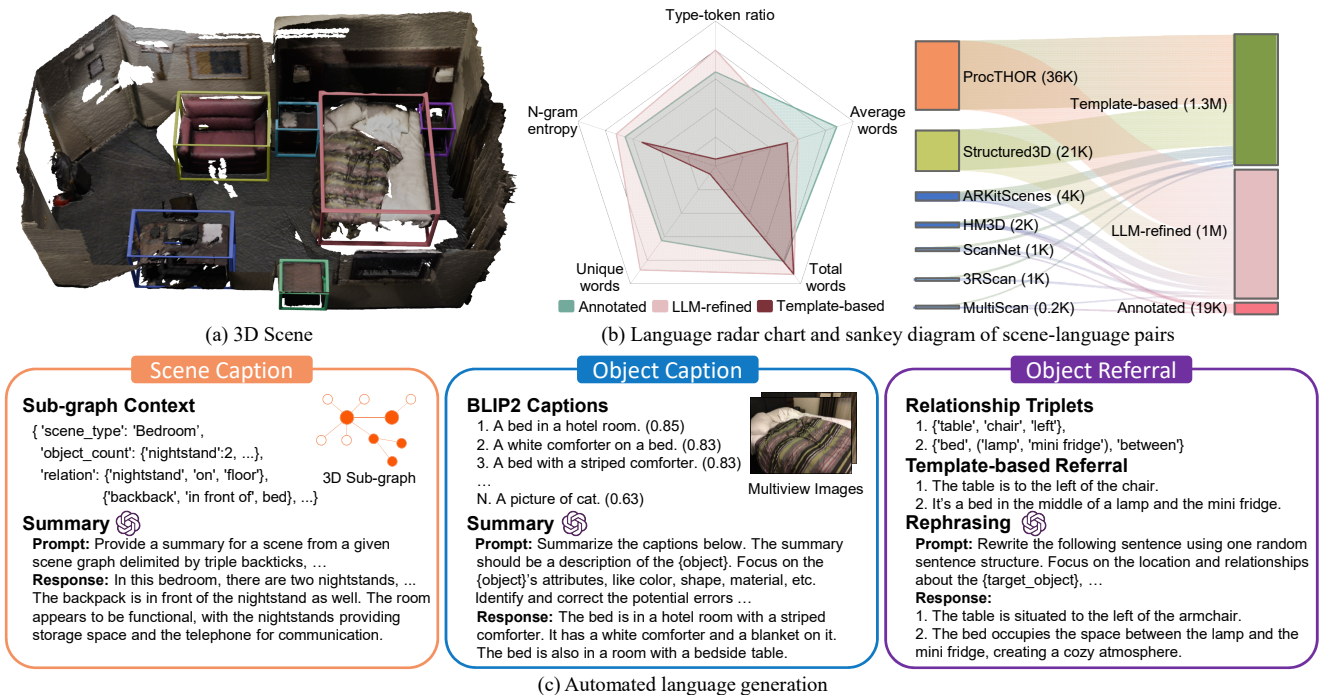


Figure 2. **SCENEVERSE collection and statistics.** Given a 3D scene (a), our automated pipeline (c) generates three types of description including **scene caption**, **object caption** and **object referral**. (b) The comparison of different language sources and data composition.

anchor object is utilized to establish the view direction. The distance between the two objects is also calculated to describe whether the objects are *far* or *near* in space.

Multi-object Relationships This models the spatial arrangement of multiple objects, *e.g.*, *align* and *between*.

The node hierarchy is decided by the *support* relationship. We traverse all the object nodes to calculate spatial relationships, which undergo an automatic verification procedure to rectify incorrect ones. For a more detailed description of the scene graph construction and relationship determination, please refer to Appendix A.2.

3.3. Language Generation with LLMs

The scene-language pairs in SCENEVERSE aim to capture varying aspects of the 3D scene, which include detailed object attribute descriptions in object captioning, spatial relationships between objects in object referral, and global scene descriptions in scene captioning. Based on the 3D scene graph, we utilize both templates and LLMs to automatically generate descriptions on these three granularities.

Object Captioning Object captions aim to provide detailed descriptions of an object’s visual and physical properties, facilitating object-level grounding with its distinctive features. Given the multi-view images, we utilize the point cloud of the object $v \in \mathcal{V}$ to identify its occurrence in the images through rendering. The images are then cropped with the rendered bounding boxes and processed through

BLIP2 [48] to generate initial object captions. To refine the captions, we select the top 10 sentences with the highest CLIP [66] similarity score and minimal occlusion. The selected sentences are fed into a LLM to obtain a coherent summary of the object captions. In this process, we explicitly instruct the language model to identify and correct the potential errors. The detailed object captioning pipeline is illustrated in Appendix A.3.

Object Referral Object relationship captions refer to objects by articulating their spatial relationships in the scene. Spatial relationship triplets (v_i, v_j, e_{ij}) are first extracted from the constructed 3D scene graph. We design various templates to generate descriptions for each relationship type, assigning the entities in the form of (*target-object*, *spatial-relation*, *anchor-object(s)*). This results in examples like “the **chair** is **next to** the **armchair**”, “facing the **sofa**, there is a **suitcase far to the right of** the **shoes**”, and “the **fridge** is **between** **cabinet** and **sofa**”. To add complexity to the template-based descriptions, we design “star-reference” templates, where the reference to the target object is generated by describing its relationship to 3 randomly chosen adjacent objects in the scene graph. Our designed templates span passive and active tenses, as well as inversion clauses, contributing to the richness of the generated text. To enhance the naturalness of the descriptions, we employ LLM for sentence rephrasing. Fig. 2 presents statistics for the descriptions before and after rephrasing.

Scene Captioning The scene-level captions emphasize global information, portraying the key objects in the scene along with their attributes and functionalities. We leverage the constructed 3D scene graph and prompt LLMs to generate these captions. To enhance the diversity of scene captions, we utilize a subgraph sampling strategy, where a subset of edges and nodes are randomly sampled as the scene context. The object counts are also provided as LLM prompts, together with the room type and object attributes if such annotations are available in the dataset.

3.4. Referral Annotation by Humans

In addition to automatically generated scene-text pairs, SCENEVERSE includes the most comprehensive set of human-annotated, context-rich object referrals to date, serving as a valuable benchmark for assessing grounded scene understanding capabilities. The human annotations contain 96,863 descriptions in ARKitScenes [9], HM3D [67] and MultiScan [58]. During the annotation process, one human annotator was assigned to write at least 20 words to distinctly refer to a single 3D object within a 3D scene. Each referral text then undergoes independent verification by two additional reviewers, both mandated to accurately locate the referenced object based on the 3D scene and the annotated referral text. Any object referrals that do not pass the verification by either reviewer are flagged for re-annotation.

3.5. Details and Statistics

In total, SCENEVERSE comprises a total of 68,406 room-level 3D scans, with the source composition shown in Fig. 2 (b). The dataset contains 1.5M object instances, comprising 21 types of relationships following prior work [1, 79]. For the language descriptions, we generate 1M template-based texts and 1M sentences by LLM rephrased by Llama [75] and GPT-3.5 [61]. All the rephrasing and summary prompts, along with the complete set of relationships, are detailed in Appendix A.3. To verify the efficacy of our automated language generation pipeline, we conduct a quality check (QC) where 12K generated object-level descriptions are randomly selected for human verification, achieving a 96.93% pass rate. This shows the capability of our proposed scene-graph-based generation approach to produce high-quality language descriptions, laying a robust foundation for future scalability.

4. Grounded Pre-training for Scenes

In this section, we introduce GPS, an efficient transformer-based model trained with multi-level contrastive losses for aligning 3D scenes and texts. As shown in Fig. 3, we echo the language descriptions collected at different levels to form scene-language pairs at both object-level, referral-object-level, and scene-level for contrastive objectives in GPS. We describe the design of each level in the following sections.

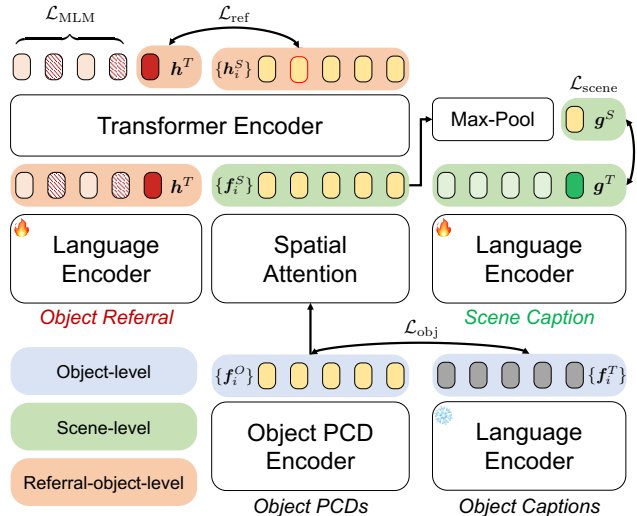


Figure 3. **Overview of our proposed GPS model.** We leverage contrastive alignment in three levels \mathcal{L}_{obj} , $\mathcal{L}_{\text{scene}}$, and \mathcal{L}_{ref} as well as a masked language modeling objective \mathcal{L}_{MLM} for model learning.

4.1. Object-level Grounding

Given a 3D scene point cloud \mathcal{S} , we use an off-the-shelf 3D object segmentation model to decompose it into a bag of N objects $\mathcal{S} = \{\mathbf{o}_1, \mathbf{o}_2, \dots, \mathbf{o}_n\}_{i=1}^N$. We extract object features $\{\mathbf{f}_i^O\}$ with an object point cloud encoder and text features $\{\mathbf{f}_i^T\}$ by feeding object-captions $\{\mathbf{T}_i^{\text{obj}}\}$ into a frozen language model. Following [83], we perform cross-modal alignment on the object features and text features via:

$$\mathcal{L}_{\text{obj}} = -\frac{1}{2} \sum_{(p,q)} \left(\log \frac{\exp(D^{\text{obj}}(p,q))}{\sum_r \exp(D^{\text{obj}}(p,r))} + \log \frac{\exp(D^{\text{obj}}(p,q))}{\sum_r \exp(D^{\text{obj}}(r,q))} \right), \quad (1)$$

where $D^{\text{obj}}(p,q) = (\mathbf{f}_p^O \mathbf{f}_q^T / \tau)$ denotes the dot product between object and text features and (p,q) denotes a pair of aligned object-text pair in the training batch and r iterates over all object-text pairs in the training batch. Similar to CLIP [66], we use a learnable temperature parameter τ to facilitate model learning.

4.2. Scene-level Grounding

With aligned object features, we encode the scene by incorporating object spatial locations into the extracted object features. Specifically, we use a spatial transformer model to encode extracted object features $\{\mathbf{f}_i^O\}$ with their spatial location features $\{\mathbf{l}_i\}$ following [18, 98]:

$$\mathbf{f}^S = \text{SpatialAttn}(\{\mathbf{f}_i^O\}, \{\mathbf{l}_i\})$$

where $\{\mathbf{f}_i^S\}$ denotes the feature of object \mathbf{o}_i after encoding with spatial location features. To perform scene-level align-

ment, we operate on these scene-level object features $\{f_i^S\}$ and align it with the scene caption T^{scene} . Specifically, we feed the object features into a projection layer and use max-pooling over all object features to obtain the scene feature g^S . Similar to object-level grounding, we pass the scene caption through a tunable language model to obtain text feature g^T and perform scene-level contrastive alignment through:

$$\mathcal{L}_{\text{scene}} = -\frac{1}{2} \sum_{(p,q)} \left(\log \frac{\exp(D^{\text{scene}}(p,q))}{\sum_r \exp(D^{\text{scene}}(p,r))} + \log \frac{\exp(D^{\text{scene}}(p,q))}{\sum_r \exp(D^{\text{scene}}(r,q))} \right), \quad (2)$$

where $D^{\text{scene}}(p,q) = (g_p^S g_q^T / \tau)$ denotes the dot product between scene feature g_p^S and scene caption feature g_q^T for each pair of aligned scene-text pairs in the training batch and r iterates over all scene-text pairs in the training batch.

4.3. Referral-object-level Grounding

To model the relationships revealed in referring expressions, we employ a self-attention-based reasoning transformer for grounding object referrals in scenes. This transformer takes in scene-object features $\{f_i^S\}$ and an object referral T^{ref} and performs self-attention to learn relationships between text descriptions and object relationships. We use the same tunable language encoder as in scene-level grounding for extracting per-object referral features. We pass this text feature together with scene-object features into the self-attention transformer to obtain the aligned object features h_i^S and the sentence-level referral feature h^T . We then perform the referral-object-level contrastive alignment following:

$$\mathcal{L}_{\text{ref}} = -\log \frac{\exp(\bar{h}^S h^T / \tau)}{\sum_p \exp(h_p^S h^T / \tau)}, \quad (3)$$

where \bar{h}^S denotes the feature of the referred object, p iterates over all objects within the same scene. Notably, in contrast to inter-scene contrast that was done in object- and scene-level alignment, we force the selection of positive pairs to be within the same scene to provide intra-scene contrast for fine-grained object grounding. This mimics the success of intra-image and inter-image contrasts commonly used for region-word alignment in 2D-VL models [90].

To learn the multi-level alignment between 3D scenes and language, we first train the point cloud encoder with object-level grounding objects to obtain a good feature initialization for grounding objects in scenes. During the scene grounding stage, we train our inter- and intra-scene objectives together with a mask language modeling loss \mathcal{L}_{MLM} over the inputted object-referral texts to tune the parameters within the language encoder and self-attention transformer. Above all, the learning of GPS could be summarized as optimizing the following objective:

$$\mathcal{L} = \mathcal{L}_{\text{obj}} + \mathcal{L}_{\text{scene}} + \mathcal{L}_{\text{ref}} + \mathcal{L}_{\text{MLM}}.$$

5. Experiments

In this section, we present the evaluation results addressing the following questions:

- How effective is the data scaling in SCENEVERSE for 3D visual grounding? Does the scale-up work for general pre-training based 3D-VL models?
- How well is the GPS pre-training pipeline? Does it exhibit similar properties of 2D-VL models in 3D-VL tasks?
- What potentials are offered by SCENEVERSE and GPS for future research? What is missing?

In the following sections, we describe in detail about model performance regarding these key topics. Due to the page limit, we direct readers to the Appendices B and C for implementation details and more experimental analyses.

5.1. 3D Visual Grounding

Settings We evaluate our model on three commonly-used datasets for 3D visual grounding: ScanRefer [16], Nr3D, and Sr3D [1]. For Nr3D and Sr3D, we follow Achlioptas *et al.* [1] and report the grounding accuracies of models using ground-truth object masks. For ScanRefer, we follow Zhu *et al.* [98] and use Mask3D [72] to generate object proposals. Results are reported as Acc@0.5 to evaluate the correctness of predictions whose object bounding boxes overlap the ground truth with IoU > 0.5. For comparisons, we compare with existing baselines by providing the results of pre-trained GPS and dataset-specific fine-tuned GPS. Please see more details in the Appendix C.

Results and Analyses As shown in Tab. 2, GPS trained on SCENEVERSE achieves state-of-the-art results on all existing 3D-VL grounding benchmarks. Initially, when GPS is trained directly on the training sets of benchmark datasets, labeled as Ours (*scratch*), it underperforms compared to existing models that employ more complex structures or loss designs. This result underscores the data-intensive nature of the contrastive alignment paradigm. However, when presented with extensive training data in SCENEVERSE, the results of our model without additional fine-tuning, *i.e.*, Ours (*pre-train*), significantly improves and already achieves state-of-the-art results on benchmarks like ScanRefer. Moreover, the dataset-specific fine-tuned model, *i.e.*, Ours (*fine-tuned*), consistently outperforms existing baselines with only a simple projection MLP added on top of the pre-trained model, jointly optimized during fine-tuning without any other auxiliary architecture or loss objective. These results underscore the strong potential of both the SCENEVERSE and GPS for 3D-VL tasks.

5.2. Zero-Shot Transfer

Settings To better evaluate the effectiveness of both the SCENEVERSE data and the GPS model, we further perform zero-shot transfer experiments to test the models' capabil-

Table 2. **3D Visual Grounding results on Nr3D, Sr3D, and ScanRefer.** We use “*direct*” for our model trained on SCENEVERSE with no additional fine-tune head, and “*fine-tune*” for the data-specific fine-tuned version of our model. We highlight the best results in **bold**.

Method	Nr3D					Sr3D					ScanRefer Acc@0.5		
	Overall	Easy	Hard	V-Dep.	V-Indep.	Overall	Easy	Hard	V-Dep.	V-Indep.	Overall	Unique	Multiple
3DVG-Trans [94]	40.8	48.5	34.8	34.8	43.7	51.4	54.2	44.9	44.6	51.7	34.7	60.6	28.4
TGNN [39]	37.3	44.2	30.6	35.8	38.0	45.0	48.5	36.9	45.8	45.0	29.7	56.8	23.2
TransRefer3D [35]	48.0	56.7	39.6	42.5	50.7	57.4	60.5	50.2	49.9	57.7	-	-	-
InstanceRefer [89]	38.8	46.0	31.8	34.5	41.9	48.0	51.1	40.5	45.8	48.1	32.9	66.8	24.7
FFL-3DOG [31]	41.7	48.2	35.0	37.1	44.7	-	-	-	-	-	34.0	67.9	25.7
LAR [6]	48.9	58.4	42.3	47.4	52.1	59.4	63.0	51.2	50.0	59.1	-	-	-
SAT [86]	56.5	64.9	48.4	54.4	57.6	57.9	61.2	50.0	49.2	58.3	30.1	50.8	25.2
3D-SPS [54]	51.5	58.1	45.1	48.0	53.2	62.6	56.2	65.4	49.2	63.2	37.0	66.7	29.8
3DJCG [12]	-	-	-	-	-	-	-	-	-	-	37.3	64.3	30.8
BUTD-DETR [41]	54.6	60.7	48.4	46.0	58.0	67.0	68.6	63.2	53.0	67.6	39.8	66.3	35.1
MVT [40]	59.5	67.4	52.7	59.1	60.3	64.5	66.9	58.8	58.4	64.7	33.3	66.5	25.3
ViL3DRel [18]	64.4	70.2	57.4	62.0	64.5	72.8	74.9	67.9	63.8	73.2	37.7	68.6	30.7
EDA [82]	52.1	58.2	46.1	50.2	53.1	68.1	70.3	62.9	54.1	68.7	42.3	68.6	37.6
3D-VisTA (<i>scratch</i>) [98]	57.5	65.9	49.4	53.7	59.4	69.6	72.1	63.6	57.9	70.1	41.5	70.9	34.8
3D-VisTA [98]	64.2	72.1	56.7	61.5	65.1	76.4	78.8	71.3	58.9	77.3	45.8	75.1	39.1
Ours (<i>scratch</i>)	58.7	67.0	50.9	55.8	59.8	68.4	70.5	63.4	53.1	69.0	40.4	71.3	34.7
Ours (<i>pre-train</i>)	55.2	62.8	48.0	45.5	58.8	74.1	76.4	68.5	54.1	75.0	47.1	77.4	41.6
Ours (<i>fine-tuned</i>)	64.9	72.5	57.8	56.9	67.9	77.5	80.1	71.6	62.8	78.2	48.1	77.9	42.7

Table 3. **Zero-shot transfer results on established benchmarks.**

Method	Nr3D	Sr3D	ScanRefer@0.25	ScanRefer@0.5
3D-VisTA (<i>scratch</i>)	57.5	69.6	45.9	41.5
3D-VisTA (<i>zero-shot</i>)	35.2	31.2	33.2	29.6
3D-VisTA (<i>zero-shot text</i>)	43.1	36.1	41.1	36.4
Ours (<i>scratch</i>)	58.7	68.4	44.5	40.4
Ours (<i>zero-shot</i>)	32.4	33.3	35.2	31.1
Ours (<i>zero-shot text</i>)	41.9	38.1	40.7	35.8

ity in 4 benchmarks, ScanRefer, Sr3D, Nr3D, and SCENEVERSE-val. We create SCENEVERSE-val using 8.5K annotated object referrals of 271 scenes in MultiScan, and randomly split the scenes following a 4:1 train / test split for creating the held-out test set. We mainly consider 2 specific transfer settings in our experiments: (i) *zero-shot*: models trained by removing all the scenes from the target dataset, tested on held-out unseen scenes, and (ii) *zero-shot text*: Models trained on data that include the 3D scenes from training set of the target dataset, yet tested exclusively with unseen scene-text distribution. Specifically, for the *zero-shot text* setting, we use the generated texts in SCENEVERSE as fine-tuning sources for the *zero-shot* model. We mainly compare our model against a recent pre-training-based model 3D-VisTA. See more details on experimental setting and implementation in the Appendix C.

Results and Analyses We present the results of zero-shot transfer experiments in Tab. 3 and Tab. 4 with the following key observations:

- Our GPS model demonstrates superior generalization to unseen scenes compared to the 3D-VisTA model. In zero-shot transfer scenarios, our model consistently outperforms 3D-VisTA across established benchmarks and

Table 4. **Zero-shot transfer on SCENEVERSE-val.** We evaluate models following settings in Nr3D/Sr3D using GT object proposals.

Method	Overall	Easy	Hard	V-Dep.	V-Indep.
3D-VisTA (<i>scratch</i>)	40.7	53.1	21.6	37.3	44.3
3D-VisTA (<i>zero-shot</i>)	52.9	59.6	35.4	53.7	52.2
3D-VisTA (<i>zero-shot text</i>)	58.1	70.0	39.6	52.5	64.1
Ours (<i>scratch</i>)	38.5	50.2	20.8	33.7	43.9
Ours (<i>zero-shot</i>)	59.2	69.4	44.0	53.1	66.3
Ours (<i>zero-shot text</i>)	60.6	70.9	45.1	54.8	67.3

SCENEVERSE-val. This indicates the effectiveness of contrastive alignment over traditional classification objectives, aligning with the advancements seen in 2D-VL models for open-vocabulary grounding and transfer capabilities

- SCENEVERSE dataset substantially enhances 3D-VL grounding capabilities through zero-shot transfer, especially when provided with relatively limited training data, *i.e.*, SCENEVERSE-val. As demonstrated in Tab. 4, there is a significantly improved performance when comparing models trained on SCENEVERSE in a zero-shot manner to those trained from scratch. This indicates that SCENEVERSE can effectively capture knowledge for general 3D scene grounding. Consequently, *this underscores its potential as a go-to pre-training dataset for 3D-VL tasks.*
- The impact of our extensive collection and scalable generation of scene-text pairs is further evidenced by the results in the *zero-shot text* setting. Notably, as shown in Tab. 3, these automatically generated scene-text pairs supply ample knowledge for comprehending the scene distribution. This contributes significantly to the substantial improvement over the *zero-shot* performance.

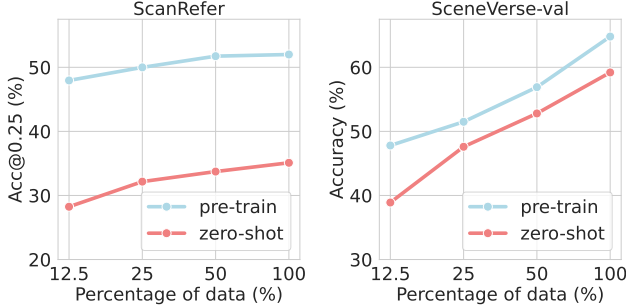


Figure 4. **Model performance v.s. data scale.** Models consistently improve in both the pre-train and zero-shot transfer settings on ScanRefer and SCENEVERSE-val with data scaling-up.

5.3. Ablative Studies and Discussions

In this section, we present ablative studies focused primarily on the data collected in SCENEVERSE. Our aim is to elucidate the effects of data scaling more clearly. For discussions regarding ablative studies on model architecture, readers are referred to the Appendix D. The following points are specifically discussed in this section.

How important is data-scaling? We conduct ablation studies over the amount of data used while pre-training GPS. We consider the model trained with $\frac{1}{8}$, $\frac{1}{4}$, $\frac{1}{2}$ of SCENEVERSE to show the effectiveness of data-scaling on model performance in the pre-train and zero-shot transfer settings in ScanRefer and SCENEVERSE-val. As shown in Fig. 4, we observe consistent performance improvement over the increase of data scale for both settings. We provide additional experiments in the Appendix D to show that such scaling effect is not only beneficial for 3D-VL grounding but also for other 3D tasks like semantic segmentation [72, 85].

How is the generated data compared with human-annotated data? We assess the performance of models trained using various scene-text sources, specifically focusing on their performance in the ScanRefer dataset without additional fine-tuning. As shown in Tab. 5, models trained with our template-based generated texts and Large Language Model (LLM)-refined texts show significant improvements over models trained solely on ScanRefer. More importantly, these variants of our model already achieve state-of-the-art results compared with previous baselines. This indicates the effectiveness of our text-generation pipeline. Finally, we observe that adding human-annotated data is still beneficial for model performance. However, the improvement is relatively marginal over models trained on our generated data.

What is the role of the synthetic scenes in this scale-up process? With synthetic data providing large-scale and diverse scene data for 3D-VL tasks, we evaluate the models’ domain transfer (Sim2Real) capability. Specifically, we compare models trained on all real scenes in SCENEVERSE against models trained exclusively on two synthetic sub-

Table 5. **Ablation on scene-text pair types used in training.** We report model results on ScanRefer with no additional finetuning.

Template	LLM	Anno.	Acc@0.25	Acc@0.5
✗	✗	✗	43.5	38.4
✓	✗	✗	50.9	46.1
✓	✓	✗	51.1	46.3
✓	✓	✓	52.0	47.1

Table 6. **Cross domain transfer results** of models learned in real and synthetic datasets without additional fine-tuning. “S3D” stands for Structured3D.

Real	Synthetic	SCENEVERSE-val	S3D	ProcTHOR
All	✗	64.8	37.1	43.4
✗	S3D	7.0	85.1	16.1
✗	ProcTHOR	4.2	16.3	91.0

sets of SCENEVERSE, *i.e.*, Structured3D and ProcTHOR. As shown in Tab. 6, models trained on synthetic subsets demonstrate remarkable performance on their corresponding test sets while suffering when transferred to real or other synthetic scenes. In contrast, the model trained on real scene-text pairs exhibits less severe performance drops when generalizing to synthetic scenes. This result affirms the domain gap between real and synthetic scenes in 3D-VL grounding and shows that a simple scale-up in the amount of scenes is insufficient when the scene naturalness can not be guaranteed. Considering the scalability of our quality-ensured language generation and also the scaling effect shown in our experiments, the rate-determining step for further scaling-up 3D-VL comes to the collection of diverse, high-quality, and realistic scenes that capture natural 3D scene distributions.

6. Conclusion

In this work, we scale up 3D-VL in the context of grounded scene understanding. We introduce SCENEVERSE, a million-scale 3D-VL dataset encompassing various scenes and multi-level scene descriptions sourced from both human annotation and our proposed scene-text generation approach. Utilizing SCENEVERSE, we propose Grounded Pre-training for Scenes, a model trained with multi-level scene-language contrastive alignment over the data collected. Through extensive experiments, we show that GPS achieves state-of-the-art results on all existing 3D-VL grounding tasks. We further conduct zero-shot transfer experiments to show the improved generalization performances of GPS trained on SCENEVERSE compared with previous baselines. We hope our efforts and successful scale-up attempts in SCENEVERSE could pave the way for a new research paradigm in 3D-VL.

7. Acknowledgement

The authors thank Yaowei Zhang from BIGAI for designing the result visualization framework, Jianguo Huang and Xiongkun Linghu from BIGAI for suggestions on data generation and refinement, and colleagues from BIGAI for their helpful discussions and suggestions.

References

- [1] Panos Achlioptas, Ahmed Abdelreheem, Fei Xia, Mohamed Elhoseiny, and Leonidas Guibas. Referit3d: Neural listeners for fine-grained 3d object identification in real-world scenes. In *Proceedings of European Conference on Computer Vision (ECCV)*, 2020. 2, 3, 5, 6, 1
- [2] Christopher Agia, Krishna Murthy Jatavallabhula, Mohamed Khodeir, Ondrej Miksik, Vibhav Vineet, Mustafa Mukadam, Liam Paull, and Florian Shkurti. Taskography: Evaluating robot task planning over large 3d scene graphs. In *Proceedings of Conference on Robot Learning (CoRL)*, 2022. 3
- [3] Jean-Baptiste Alayrac, Jeff Donahue, Pauline Luc, Antoine Miech, Iain Barr, Yana Hasson, Karel Lenc, Arthur Mensch, Katherine Millican, Malcolm Reynolds, et al. Flamingo: a visual language model for few-shot learning. In *Proceedings of Advances in Neural Information Processing Systems (NeurIPS)*, 2022. 2, 3
- [4] Iro Armeni, Zhi-Yang He, JunYoung Gwak, Amir R Zamir, Martin Fischer, Jitendra Malik, and Silvio Savarese. 3d scene graph: A structure for unified semantics, 3d space, and camera. In *Proceedings of International Conference on Computer Vision (ICCV)*, 2019. 2, 3
- [5] Daichi Azuma, Taiki Miyayoshi, Shuhei Kurita, and Motoaki Kawanabe. Scanqa: 3d question answering for spatial scene understanding. In *Proceedings of Conference on Computer Vision and Pattern Recognition (CVPR)*, 2022. 2, 3
- [6] Eslam Bakr, Yasmien Alsaedy, and Mohamed Elhoseiny. Look around and refer: 2d synthetic semantics knowledge distillation for 3d visual grounding. In *Proceedings of Advances in Neural Information Processing Systems (NeurIPS)*, 2022. 3, 7
- [7] Lawrence W Barsalou. Perceptual symbol systems. *Behavioral and brain sciences*, 22(4):577–660, 1999. 2
- [8] Lawrence W Barsalou. Grounded cognition. *Annu. Rev. Psychol.*, 59:617–645, 2008. 2
- [9] Gilad Baruch, Zhuoyuan Chen, Afshin Dehghan, Tal Dimry, Yuri Feigin, Peter Fu, Thomas Gebauer, Brandon Joffe, Daniel Kurz, Arik Schwartz, et al. Arkitscenes: A diverse real-world dataset for 3d indoor scene understanding using mobile rgb-d data. In *Proceedings of Advances in Neural Information Processing Systems Datasets and Benchmarks (NeurIPS Datasets and Benchmarks Track)*, 2021. 2, 3, 5, 1
- [10] Rishi Bommasani, Drew A Hudson, Ehsan Adeli, Russ Altman, Simran Arora, Sydney von Arx, Michael S Bernstein, Jeannette Bohg, Antoine Bosselut, Emma Brunskill, et al. On the opportunities and risks of foundation models. *arXiv preprint arXiv:2108.07258*, 2021. 2
- [11] Tom Brown, Benjamin Mann, Nick Ryder, Melanie Subbiah, Jared D Kaplan, Prafulla Dhariwal, Arvind Neelakantan, Pranav Shyam, Girish Sastry, Amanda Askell, et al. Language models are few-shot learners. In *Proceedings of Advances in Neural Information Processing Systems (NeurIPS)*, 2020. 2, 3
- [12] Daigang Cai, Lichen Zhao, Jing Zhang, Lu Sheng, and Dong Xu. 3djcg: A unified framework for joint dense captioning and visual grounding on 3d point clouds. In *Proceedings of Conference on Computer Vision and Pattern Recognition (CVPR)*, 2022. 7
- [13] Angel Chang, Angela Dai, Thomas Funkhouser, Maciej Halber, Matthias Niessner, Manolis Savva, Shuran Song, Andy Zeng, and Yinda Zhang. Matterport3d: Learning from rgb-d data in indoor environments. *Proceedings of International Conference on 3D Vision (3DV)*, 2017. 2
- [14] Angel X Chang, Thomas Funkhouser, Leonidas Guibas, Pat Hanrahan, Qixing Huang, Zimo Li, Silvio Savarese, Manolis Savva, Shuran Song, Hao Su, et al. Shapenet: An information-rich 3d model repository. *arXiv preprint arXiv:1512.03012*, 2015. 2
- [15] Soravit Changpinyo, Piyush Sharma, Nan Ding, and Radu Soricut. Conceptual 12m: Pushing web-scale image-text pre-training to recognize long-tail visual concepts. In *Proceedings of Conference on Computer Vision and Pattern Recognition (CVPR)*, 2021. 2, 3
- [16] Dave Zhenyu Chen, Angel X Chang, and Matthias Nießner. Scanrefer: 3d object localization in rgb-d scans using natural language. In *Proceedings of European Conference on Computer Vision (ECCV)*, 2020. 2, 3, 6, 1
- [17] Dave Zhenyu Chen, Qirui Wu, Matthias Nießner, and Angel X Chang. D3net: a speaker-listener architecture for semi-supervised dense captioning and visual grounding in rgb-d scans. In *Proceedings of European Conference on Computer Vision (ECCV)*, 2022. 3
- [18] Shizhe Chen, Pierre-Louis Guhur, Makarand Tapaswi, Cordelia Schmid, and Ivan Laptev. Language conditioned spatial relation reasoning for 3d object grounding. In *Proceedings of Advances in Neural Information Processing Systems (NeurIPS)*, 2022. 3, 5, 7, 1
- [19] Sijin Chen, Hongyuan Zhu, Xin Chen, Yinjie Lei, Gang Yu, and Tao Chen. End-to-end 3d dense captioning with vote2capdet. In *Proceedings of Conference on Computer Vision and Pattern Recognition (CVPR)*, 2023. 3
- [20] Zhenyu Chen, Ali Gholami, Matthias Nießner, and Angel X Chang. Scan2cap: Context-aware dense captioning in rgb-d scans. In *Proceedings of Conference on Computer Vision and Pattern Recognition (CVPR)*, 2021. 3
- [21] Zhenyu Chen, Ronghang Hu, Xinlei Chen, Matthias Nießner, and Angel X Chang. Unit3d: A unified transformer for 3d dense captioning and visual grounding. In *Proceedings of International Conference on Computer Vision (ICCV)*, 2023. 5
- [22] Jasmine Collins, Shubham Goel, Kenan Deng, Achleshwar Luthra, Leon Xu, Erhan Gundogdu, Xi Zhang, Tomas F Yago Vicente, Thomas Dideriksen, Himanshu Arora, et al. Abo: Dataset and benchmarks for real-world 3d object understanding. In *Proceedings of Conference on Computer Vision and Pattern Recognition (CVPR)*, 2022. 2
- [23] Angela Dai, Angel X Chang, Manolis Savva, Maciej Halber, Thomas Funkhouser, and Matthias Nießner. Scannet: Richly-annotated 3d reconstructions of indoor scenes. In *Proceedings*

- of Conference on Computer Vision and Pattern Recognition (CVPR), 2017. 2, 3, 1
- [24] Wenliang Dai, Junnan Li, Dongxu Li, Anthony Meng Huat Tiong, Junqi Zhao, Weisheng Wang, Boyang Li, Pascale Fung, and Steven Hoi. Instructblip: Towards general-purpose vision-language models with instruction tuning. *arXiv preprint arXiv:2305.06500*, 2023. 3
- [25] Matt Deitke, Ruoshi Liu, Matthew Wallingford, Huong Ngo, Oscar Michel, Aditya Kusupati, Alan Fan, Christian Laforte, Vikram Voleti, Samir Yitzhak Gadre, et al. Objaverse-xl: A universe of 10m+ 3d objects. In *Proceedings of Advances in Neural Information Processing Systems (NeurIPS)*, 2023. 2
- [26] Matt Deitke, Dustin Schwenk, Jordi Salvador, Luca Weihs, Oscar Michel, Eli VanderBilt, Ludwig Schmidt, Kiana Ehsani, Aniruddha Kembhavi, and Ali Farhadi. Objaverse: A universe of annotated 3d objects. In *Proceedings of Conference on Computer Vision and Pattern Recognition (CVPR)*, 2023. 2
- [27] Matt Deitke, Eli VanderBilt, Alvaro Herrasti, Luca Weihs, Kiana Ehsani, Jordi Salvador, Winson Han, Eric Kolve, Aniruddha Kembhavi, and Roozbeh Mottaghi. Prothor: Large-scale embodied ai using procedural generation. In *Proceedings of Advances in Neural Information Processing Systems (NeurIPS)*, 2022. 2, 3, 1
- [28] Jacob Devlin, Ming-Wei Chang, Kenton Lee, and Kristina Toutanova. Bert: Pre-training of deep bidirectional transformers for language understanding. In *Proceedings of Conference of the North American Chapter of the Association for Computational Linguistics (NAACL)*, 2018. 3
- [29] Runyu Ding, Jihan Yang, Chuhui Xue, Wenqing Zhang, Song Bai, and Xiaojuan Qi. Pla: Language-driven open-vocabulary 3d scene understanding. In *Proceedings of Conference on Computer Vision and Pattern Recognition (CVPR)*, 2023. 3
- [30] Zhipeng Ding, Xu Han, and Marc Niethammer. Votenet: A deep learning label fusion method for multi-atlas segmentation. In *Proceedings of International Conference on Medical Image Computing and Computer-Assisted Intervention (MICCAI)*, 2019. 3
- [31] Mingtao Feng, Zhen Li, Qi Li, Liang Zhang, XiangDong Zhang, Guangming Zhu, Hui Zhang, Yaonan Wang, and Ajmal Mian. Free-form description guided 3d visual graph network for object grounding in point cloud. In *Proceedings of International Conference on Computer Vision (ICCV)*, 2021. 7
- [32] Golnaz Ghiasi, Xiuye Gu, Yin Cui, and Tsung-Yi Lin. Scaling open-vocabulary image segmentation with image-level labels. In *Proceedings of European Conference on Computer Vision (ECCV)*, 2022. 3
- [33] Qiao Gu, Alihusein Kuwajerwala, Sacha Morin, Krishna Murthy Jatavallabhula, Bipasha Sen, Aditya Agarwal, Corban Rivera, William Paul, Kirsty Ellis, Rama Chellappa, et al. Conceptgraphs: Open-vocabulary 3d scene graphs for perception and planning. *arXiv preprint arXiv:2309.16650*, 2023. 3
- [34] Huy Ha and Shuran Song. Semantic abstraction: Open-world 3d scene understanding from 2d vision-language models. In *Proceedings of Conference on Robot Learning (CoRL)*, 2022. 3
- [35] Dailan He, Yusheng Zhao, Junyu Luo, Tianrui Hui, Shaofei Huang, Aixi Zhang, and Si Liu. Transrefer3d: Entity-and-relation aware transformer for fine-grained 3d visual grounding. In *Proceedings of ACM International Conference on Multimedia (MM)*, 2021. 3, 7
- [36] Deepthi Hegde, Jeya Maria Jose Valanarasu, and Vishal Patel. Clip goes 3d: Leveraging prompt tuning for language grounded 3d recognition. In *Proceedings of International Conference on Computer Vision (ICCV)*, 2023. 3, 1
- [37] Yining Hong, Chunru Lin, Yilun Du, Zhenfang Chen, Joshua B Tenenbaum, and Chuang Gan. 3d concept learning and reasoning from multi-view images. In *Proceedings of Conference on Computer Vision and Pattern Recognition (CVPR)*, 2023. 3
- [38] Yicong Hong, Qi Wu, Yuankai Qi, Cristian Rodriguez-Opazo, and Stephen Gould. Vln bert: A recurrent vision-and-language bert for navigation. In *Proceedings of Conference on Computer Vision and Pattern Recognition (CVPR)*, 2021. 3
- [39] Pin-Hao Huang, Han-Hung Lee, Hwann-Tzong Chen, and Tyng-Luh Liu. Text-guided graph neural networks for referring 3d instance segmentation. In *Proceedings of AAAI Conference on Artificial Intelligence (AAAI)*, 2021. 7
- [40] Shijia Huang, Yilun Chen, Jiaya Jia, and Liwei Wang. Multi-view transformer for 3d visual grounding. In *Proceedings of Conference on Computer Vision and Pattern Recognition (CVPR)*, 2022. 2, 3, 7
- [41] Ayush Jain, Nikolaos Gkanatsios, Ishita Mediratta, and Kateřina Fragkiadaki. Bottom up top down detection transformers for language grounding in images and point clouds. In *Proceedings of European Conference on Computer Vision (ECCV)*, 2022. 3, 7
- [42] Li Jiang, Hengshuang Zhao, Shaoshuai Shi, Shu Liu, Chi-Wing Fu, and Jiaya Jia. Pointgroup: Dual-set point grouping for 3d instance segmentation. In *Proceedings of Conference on Computer Vision and Pattern Recognition (CVPR)*, 2020. 3
- [43] Jared Kaplan, Sam McCandlish, Tom Henighan, Tom B Brown, Benjamin Chess, Rewon Child, Scott Gray, Alec Radford, Jeffrey Wu, and Dario Amodei. Scaling laws for neural language models. *arXiv preprint arXiv:2001.08361*, 2020. 3
- [44] Alexander Kirillov, Eric Mintun, Nikhila Ravi, Hanzi Mao, Chloe Rolland, Laura Gustafson, Tete Xiao, Spencer Whitehead, Alexander C Berg, Wan-Yen Lo, et al. Segment anything. In *Proceedings of International Conference on Computer Vision (ICCV)*, 2023. 3
- [45] Ranjay Krishna, Yuke Zhu, Oliver Groth, Justin Johnson, Kenji Hata, Joshua Kravitz, Stephanie Chen, Yannis Kalantidis, Li-Jia Li, David A Shamma, et al. Visual genome: Connecting language and vision using crowdsourced dense image annotations. In *International Journal of Computer Vision (IJCV)*, 2017. 2
- [46] Brenden M Lake, Tomer D Ullman, Joshua B Tenenbaum, and Samuel J Gershman. Building machines that learn and think like people. *Behavioral and brain sciences*, 40:e253, 2017. 2
- [47] Boyi Li, Kilian Q Weinberger, Serge Belongie, Vladlen Koltun, and Rene Ranftl. Language-driven semantic segmentation. In *Proceedings of International Conference on Learning Representations (ICLR)*, 2022. 3

- [48] Junnan Li, Dongxu Li, Silvio Savarese, and Steven Hoi. BLIP-2: bootstrapping language-image pre-training with frozen image encoders and large language models. In *ICML*, 2023. 4, 3, 5
- [49] Junnan Li, Dongxu Li, Caiming Xiong, and Steven Hoi. Blip: Bootstrapping language-image pre-training for unified vision-language understanding and generation. In *Proceedings of International Conference on Machine Learning (ICML)*, 2022. 3
- [50] Liunian Harold Li, Pengchuan Zhang, Haotian Zhang, Jianwei Yang, Chunyuan Li, Yiwu Zhong, Lijuan Wang, Lu Yuan, Lei Zhang, Jenq-Neng Hwang, et al. Grounded language-image pre-training. In *Proceedings of Conference on Computer Vision and Pattern Recognition (CVPR)*, 2022. 3
- [51] Haotian Liu, Chunyuan Li, Qingyang Wu, and Yong Jae Lee. Visual instruction tuning. In *Proceedings of Advances in Neural Information Processing Systems (NeurIPS)*, 2023. 2, 3
- [52] Minghua Liu, Ruoxi Shi, Kaiming Kuang, Yin hao Zhu, Xuanlin Li, Shizhong Han, Hong Cai, Fatih Porikli, and Hao Su. Openshape: Scaling up 3d shape representation towards open-world understanding. *arXiv preprint arXiv:2305.10764*, 2023. 2
- [53] Ruoshi Liu, Rundi Wu, Basile Van Hoorick, Pavel Tokmakov, Sergey Zakharov, and Carl Vondrick. Zero-1-to-3: Zero-shot one image to 3d object. In *Proceedings of International Conference on Computer Vision (ICCV)*, 2023. 2
- [54] Junyu Luo, Jiahui Fu, Xianghao Kong, Chen Gao, Haibing Ren, Hao Shen, Huaxia Xia, and Si Liu. 3d-sps: Single-stage 3d visual grounding via referred point progressive selection. In *Proceedings of Conference on Computer Vision and Pattern Recognition (CVPR)*, 2022. 3, 7
- [55] Tiange Luo, Chris Rockwell, Honglak Lee, and Justin Johnson. Scalable 3d captioning with pretrained models. In *Proceedings of Advances in Neural Information Processing Systems (NeurIPS)*, 2023. 2, 3
- [56] Chih-Yao Ma, Jiasen Lu, Zuxuan Wu, Ghassan AlRegib, Zolt Kira, Richard Socher, and Caiming Xiong. Self-monitoring navigation agent via auxiliary progress estimation. In *Proceedings of International Conference on Learning Representations (ICLR)*, 2019. 3
- [57] Xiaojian Ma, Silong Yong, Zilong Zheng, Qing Li, Yitao Liang, Song-Chun Zhu, and Siyuan Huang. Sqa3d: Situated question answering in 3d scenes. In *Proceedings of International Conference on Learning Representations (ICLR)*, 2023. 3
- [58] Yongsen Mao, Yiming Zhang, Hanxiao Jiang, Angel Chang, and Manolis Savva. Multiscan: Scalable rgb-d scanning for 3d environments with articulated objects. In *Proceedings of Advances in Neural Information Processing Systems (NeurIPS)*, 2022. 2, 3, 5, 1
- [59] Ishan Misra, Rohit Girdhar, and Armand Joulin. An end-to-end transformer model for 3d object detection. In *Proceedings of International Conference on Computer Vision (ICCV)*, 2021. 3
- [60] Kaichun Mo, Shilin Zhu, Angel X Chang, Li Yi, Subarna Tripathi, Leonidas J Guibas, and Hao Su. Partnet: A large-scale benchmark for fine-grained and hierarchical part-level 3d object understanding. In *Proceedings of Conference on Computer Vision and Pattern Recognition (CVPR)*, 2019. 2
- [61] OpenAI. Introducing chatgpt. <https://openai.com/blog/chatgpt>, 2022. 5
- [62] OpenAI. Gpt-4 technical report. *arXiv preprint arXiv:2303.08774*, 2023. 3
- [63] Alexander Pashevich, Cordelia Schmid, and Chen Sun. Episodic transformer for vision-and-language navigation. In *Proceedings of International Conference on Computer Vision (ICCV)*, 2021. 3
- [64] Songyou Peng, Kyle Genova, Chiyu Jiang, Andrea Tagliaschi, Marc Pollefeys, Thomas Funkhouser, et al. Openscene: 3d scene understanding with open vocabularies. In *Proceedings of Conference on Computer Vision and Pattern Recognition (CVPR)*, 2023. 3
- [65] Charles Ruizhongtai Qi, Li Yi, Hao Su, and Leonidas J Guibas. Pointnet++: Deep hierarchical feature learning on point sets in a metric space. In *Proceedings of Advances in Neural Information Processing Systems (NeurIPS)*, 2017. 1, 5
- [66] Alec Radford, Jong Wook Kim, Chris Hallacy, Aditya Ramesh, Gabriel Goh, Sandhini Agarwal, Girish Sastry, Amanda Askell, Pamela Mishkin, Jack Clark, et al. Learning transferable visual models from natural language supervision. In *International conference on machine learning*, pages 8748–8763. PMLR, 2021. 2, 3, 4, 5
- [67] Santhosh K Ramakrishnan, Aaron Gokaslan, Erik Wijmans, Oleksandr Maksymets, Alex Clegg, John Turner, Eric Urdzander, Wojciech Galuba, Andrew Westbury, Angel X Chang, et al. Habitat-matterport 3d dataset (hm3d): 1000 large-scale 3d environments for embodied ai. In *Proceedings of Advances in Neural Information Processing Systems Datasets and Benchmarks (NeurIPS Datasets and Benchmarks Track)*, 2021. 2, 3, 5, 1
- [68] Krishan Rana, Jesse Haviland, Sourav Garg, Jad Abou-Chakra, Ian Reid, and Niko Suenderhauf. Sayplan: Grounding large language models using 3d scene graphs for scalable robot task planning. In *Proceedings of Conference on Robot Learning (CoRL)*, 2023. 3
- [69] Antoni Rosinol, Andrew Violette, Marcus Abate, Nathan Hughes, Yun Chang, Jingnan Shi, Arjun Gupta, and Luca Carlone. Kimera: From slam to spatial perception with 3d dynamic scene graphs. *International Journal of Robotics Research (IJRR)*, 2021. 3
- [70] Chitwan Saharia, William Chan, Saurabh Saxena, Lala Li, Jay Wang, Emily L Denton, Kamyar Ghasemipour, Raphael Gontijo Lopes, Burcu Karagol Ayan, Tim Salimans, et al. Photorealistic text-to-image diffusion models with deep language understanding. *Proceedings of Advances in Neural Information Processing Systems (NeurIPS)*, 2022. 3
- [71] Christoph Schuhmann, Romain Beaumont, Richard Vencu, Cade Gordon, Ross Wightman, Mehdi Cherti, Theo Coombes, Aarush Katta, Clayton Mullis, Mitchell Wortsman, et al. Laion-5b: An open large-scale dataset for training next generation image-text models. In *Proceedings of Advances in Neural Information Processing Systems (NeurIPS)*, 2022. 2, 3
- [72] Jonas Schult, Francis Engelmann, Alexander Hermans, Or Litany, Siyu Tang, and Bastian Leibe. Mask3d: Mask transformer for 3d semantic instance segmentation. In *Proceed-*

- ings of *International Conference on Robotics and Automation (ICRA)*, 2023. 3, 6, 8
- [73] Linda Smith and Michael Gasser. The development of embodied cognition: Six lessons from babies. *Artificial life*, 11(1-2):13–29, 2005. 2
- [74] Ayça Takmaz, Elisabetta Fedele, Robert W Sumner, Marc Pollefeys, Federico Tombari, and Francis Engelmann. Openmask3d: Open-vocabulary 3d instance segmentation. In *Proceedings of Advances in Neural Information Processing Systems (NeurIPS)*, 2023. 3
- [75] Hugo Touvron, Thibaut Lavril, Gautier Izacard, Xavier Martinet, Marie-Anne Lachaux, Timothée Lacroix, Baptiste Rozière, Naman Goyal, Eric Hambro, Faisal Azhar, et al. Llama: Open and efficient foundation language models. *arXiv preprint arXiv:2302.13971*, 2023. 2, 5
- [76] Maria Tsimpoukelli, Jacob L Menick, Serkan Cabi, SM Eslami, Oriol Vinyals, and Felix Hill. Multimodal few-shot learning with frozen language models. *Proceedings of Advances in Neural Information Processing Systems (NeurIPS)*, 2021. 3
- [77] Thang Vu, Kookhoi Kim, Tung M Luu, Thanh Nguyen, and Chang D Yoo. Softgroup for 3d instance segmentation on point clouds. In *Proceedings of Conference on Computer Vision and Pattern Recognition (CVPR)*, 2022. 3
- [78] Johanna Wald, Armen Avetisyan, Nassir Navab, Federico Tombari, and Matthias Nießner. Rio: 3d object instance re-localization in changing indoor environments. In *Proceedings of International Conference on Computer Vision (ICCV)*, 2019. 2, 3, 1
- [79] Johanna Wald, Helisa Dhama, Nassir Navab, and Federico Tombari. Learning 3d semantic scene graphs from 3d indoor reconstructions. In *Proceedings of Conference on Computer Vision and Pattern Recognition (CVPR)*, 2020. 2, 3, 5
- [80] Xin Wang, Qiuyuan Huang, Asli Celikyilmaz, Jianfeng Gao, Dinghan Shen, Yuan-Fang Wang, William Yang Wang, and Lei Zhang. Reinforced cross-modal matching and self-supervised imitation learning for vision-language navigation. In *Proceedings of Conference on Computer Vision and Pattern Recognition (CVPR)*, 2019. 3
- [81] Tong Wu, Jiarui Zhang, Xiao Fu, Yuxin Wang, Jiawei Ren, Liang Pan, Wayne Wu, Lei Yang, Jiaqi Wang, Chen Qian, et al. Omniobject3d: Large-vocabulary 3d object dataset for realistic perception, reconstruction and generation. In *Proceedings of Conference on Computer Vision and Pattern Recognition (CVPR)*, 2023. 2
- [82] Yanmin Wu, Xinhua Cheng, Renrui Zhang, Zesen Cheng, and Jian Zhang. Eda: Explicit text-decoupling and dense alignment for 3d visual grounding. In *Proceedings of Conference on Computer Vision and Pattern Recognition (CVPR)*, 2023. 3, 7
- [83] Le Xue, Mingfei Gao, Chen Xing, Roberto Martín-Martín, Jiajun Wu, Caiming Xiong, Ran Xu, Juan Carlos Niebles, and Silvio Savarese. Ulip: Learning a unified representation of language, images, and point clouds for 3d understanding. In *Proceedings of Conference on Computer Vision and Pattern Recognition (CVPR)*, 2023. 2, 3, 5
- [84] Jihan Yang, Runyu Ding, Zhe Wang, and Xiaojuan Qi. Regionplc: Regional point-language contrastive learning for open-world 3d scene understanding. *arXiv preprint arXiv:2304.00962*, 2023. 3
- [85] Yu-Qi Yang, Yu-Xiao Guo, Jian-Yu Xiong, Yang Liu, Hao Pan, Peng-Shuai Wang, Xin Tong, and Baining Guo. Swin3d: A pretrained transformer backbone for 3d indoor scene understanding. *arXiv preprint arXiv:2304.06906*, 2023. 8, 7
- [86] Zhengyuan Yang, Songyang Zhang, Liwei Wang, and Jiebo Luo. Sat: 2d semantics assisted training for 3d visual grounding. In *Proceedings of International Conference on Computer Vision (ICCV)*, 2021. 3, 7
- [87] Chandan Yeshwanth, Yueh-Cheng Liu, Matthias Nießner, and Angela Dai. Scannet++: A high-fidelity dataset of 3d indoor scenes. In *Proceedings of International Conference on Computer Vision (ICCV)*, 2023. 2
- [88] Zhihao Yuan, Xu Yan, Yinghong Liao, Yao Guo, Guanbin Li, Shuguang Cui, and Zhen Li. X-trans2cap: Cross-modal knowledge transfer using transformer for 3d dense captioning. In *Proceedings of Conference on Computer Vision and Pattern Recognition (CVPR)*, 2022. 3
- [89] Zhihao Yuan, Xu Yan, Yinghong Liao, Ruimao Zhang, Sheng Wang, Zhen Li, and Shuguang Cui. Instancerefer: Cooperative holistic understanding for visual grounding on point clouds through instance multi-level contextual referring. In *Proceedings of International Conference on Computer Vision (ICCV)*, 2021. 7
- [90] Haotian Zhang, Pengchuan Zhang, Xiaowei Hu, Yen-Chun Chen, Liunian Li, Xiyang Dai, Lijuan Wang, Lu Yuan, Jenq-Neng Hwang, and Jianfeng Gao. Glipv2: Unifying localization and vision-language understanding. In *Proceedings of Advances in Neural Information Processing Systems (NeurIPS)*, 2022. 6
- [91] Renrui Zhang, Ziyu Guo, Wei Zhang, Kunchang Li, Xupeng Miao, Bin Cui, Yu Qiao, Peng Gao, and Hongsheng Li. Pointclip: Point cloud understanding by clip. In *Proceedings of Conference on Computer Vision and Pattern Recognition (CVPR)*, 2022. 3
- [92] Renrui Zhang, Lihui Wang, Yu Qiao, Peng Gao, and Hongsheng Li. Learning 3d representations from 2d pre-trained models via image-to-point masked autoencoders. In *Proceedings of Conference on Computer Vision and Pattern Recognition (CVPR)*, 2023. 3
- [93] Yiming Zhang, ZeMing Gong, and Angel X Chang. Multi3drefer: Grounding text description to multiple 3d objects. In *Proceedings of International Conference on Computer Vision (ICCV)*, 2023. 3
- [94] Lichen Zhao, Daigang Cai, Lu Sheng, and Dong Xu. 3dvg-transformer: Relation modeling for visual grounding on point clouds. In *Proceedings of International Conference on Computer Vision (ICCV)*, 2021. 3, 7
- [95] Jia Zheng, Junfei Zhang, Jing Li, Rui Tang, Shenghua Gao, and Zihan Zhou. Structured3d: A large photo-realistic dataset for structured 3d modeling. In *Proceedings of European Conference on Computer Vision (ECCV)*, 2020. 2, 3, 1
- [96] Wanrong Zhu, Jack Hessel, Anas Awadalla, Samir Yitzhak Gadre, Jesse Dodge, Alex Fang, Youngjae Yu, Ludwig Schmidt, William Yang Wang, and Yejin Choi. Multimodal c4: An open, billion-scale corpus of images interleaved with text. *arXiv preprint arXiv:2304.06939*, 2023. 2
- [97] Yixin Zhu, Tao Gao, Lifeng Fan, Siyuan Huang, Mark Edmonds, Hangxin Liu, Feng Gao, Chi Zhang, Siyuan Qi,

Ying Nian Wu, et al. Dark, beyond deep: A paradigm shift to cognitive ai with humanlike common sense. *Engineering*, 6(3):310–345, 2020. [2](#)

- [98] Ziyu Zhu, Xiaojian Ma, Yixin Chen, Zhidong Deng, Siyuan Huang, and Qing Li. 3d-vista: Pre-trained transformer for 3d vision and text alignment. In *Proceedings of International Conference on Computer Vision (ICCV)*, 2023. [3](#), [5](#), [6](#), [7](#), [1](#)

SCENEVERSE:

Scaling 3D Vision-Language Learning for Grounded Scene Understanding

Supplementary Material

In Appendix A, we introduce more details of SCENEVERSE, including the 3D scene preprocessing, scene graph construction and automatic language generation. Appendix B presents more model and implementation details. Appendix C include a more in-depth summary of the settings and implementations for the experiments in the main paper, as well as the ablative study and additional experiments on semantic segmentation to demonstrate the benefits of SCENEVERSE.

A. SCENEVERSE

A.1. 3D Scenes

To address the scarcity of available 3D scene data, we construct SCENEVERSE by unifying 3D scene data from various existing datasets. The curation involves utilizing real-world scene datasets such as ScanNet [23], ARKitScenes [9], HM3D [67], 3RScan [78] and MultiScan [58], in conjunction with synthetic environments from Structured3D [95] and ProcTHOR [27]. The incorporation of these synthetic datasets is primarily driven by their potential as scalable data sources for 3D-VL alignment. To facilitate the training process, we conduct the following preprocessing steps.

Room Segmentation The 3D scenes in HM3D and ProcTHOR are released at the building level, encompassing multiple rooms and sometimes spanning over 50 meters. To align with existing benchmarks [1, 16], we leverage the associated metadata to segment the 3D point cloud at the room level, facilitating subsequent operations in scene graph construction and language description generation. Additionally, we implement a filtering process to exclude extremely large rooms and those with fewer than 4 objects in the scene.

Point Cloud Normalization In order to mitigate the data disparities arising from diverse capture devices across various data sources, we subsample each point cloud to a maximum of 240,000 points. Each point cloud then undergoes a transformation centered on the central point on the floor, followed by rotation to align the room layout with the axis following the approach by Chen *et al.* [18].

Semantic Label Alignment Given the divergence in semantic label sets across different datasets, we undertake a comprehensive effort to map all the object class labels to the 607 semantic labels in ScanNet [23] to facilitate close-vocabulary object classification [65] in the existing model framework [98]. We construct the mapping in each dataset through LLM and manual verification. Note that the object-level grounding in GPS can directly deal with open-set ob-

Table A.1. **Relationships in SCENEVERSE.** The 3D scene graph captures 21 types of relationships ranging in 4 categories.

Category	Relation
In-contact vertical	supported by embedded into placed in inside
Non-contact vertical	hanging on affixed on mounted on above higher than below lower than
Horizontal	near(far) to the left of near(far) to the right of is behind is in front of close to adjacent to besides next to
Multi-object	between aligned

ject labels or captions, similar to CLIP [36].

After the preprocessing, each scan is represented by a point cloud $P \in \mathbb{R}^{N \times 8}$, wherein each point is defined by its 3D coordinates, RGB color, instance id and semantic label. In total, we curate 68,406 3D scenes in SCENEVERSE.

A.2. 3D Scene Graph Construction

In Sec. 3.2, we introduce an automated pipeline to construct 3D scene graphs from point clouds. Here, we provide more implementation details and the relationship definition.

A.2.1 Relationships

Our 3D scene graph captures 21 types of relations as shown in Tab. A.1. We provide illustrations of how these relations are defined in the 3D space, as can be seen in Fig. A.1.

A.2.2 Scene Graph Construction

Due to the inherent noise and incompleteness in the point cloud representation, automatically extracting precise and comprehensive relationships from the point clouds is a non-trivial task. Below we detail our 3D scene graph construction process, as outlined in Alg. 1.

We first instantiate the graph nodes with the instance annotation from the point cloud and parameterize each node with object centroid $p_i \in \mathbb{R}^3$ and size of the axis-aligned bounding box $b_i = (b_x, b_y, b_z) \in \mathbb{R}^3$ (Line 1-3). Next, we traverse all the nodes to determine their spatial relationships (Line 4-22). Notably, in cases where an object node lacks any in-contact vertical relationships with other objects in the scene, we designate such objects as "hangable" and calculate their non-contact vertical relationships (Line 9-13). Examples of such objects include paintings, curtains, etc. Finally, we establish relationships between multiple objects (Line 23): i) When a target object is connected with two edges labeled `left` and `right`, the target object, along with the two neighboring nodes, forms a `between` relationship triplets. ii) If the offset of the center point coordinates of a group of objects in either the X-axis or Y-axis direction is smaller than a specified offset threshold δ , then this group of objects forms an `align` relationship. The offset threshold δ will be adjusted based on the size of the scene. In addition, we utilize an automatic verification procedure to validate the scene graph, further improving the quality of the scene graph we constructed (line 24). One of the verification operations involves manually maintaining a mapping between objects and relationship descriptions based on common sense. For example, people usually use "mounted on" to describe the relation between TV and wall, rather than "hanging on". Therefore, we would automatically refined (`TV, hanging on, wall`) to (`TV, mounted on, wall`).

In our constructed 3D scene graph $\mathcal{G} = (\mathcal{V}, \mathcal{E})$, the nodes \mathcal{V} comprises $\mathcal{V}_1 \cup \mathcal{V}_2 \cup \dots \cup \mathcal{V}_K$, with \mathcal{V}_k representing the set of nodes at a particular hierarchical level. The hierarchies are determined by the `support` relationship; for instance, objects supported by the floor constitute \mathcal{V}_0 , while objects supported by the table will form \mathcal{V}_1 , etc. Note that edges originating from one node $v \in \mathcal{V}_k$ may only terminate in nearby hierarchies $\mathcal{V}_k \cup \mathcal{V}_{k+1} \cup \mathcal{V}_{k-1}$. In other words, edges in the scene graph exclusively connect nodes within the same hierarchical level, or one level higher or lower.

A.3. Language Generation Details

In Sec. 3.3, we adopt both templates and LLM to automatically generate scene-language pairs in SCENEVERSE. More technical details and examples are provided in this section.

Algorithm 1: Scene Graph Construction Pipeline

Input : M object point clouds $\{P_1, P_2, \dots, P_m\}$

Output : 3D scene graph $\mathcal{G}(\mathcal{V}, \mathcal{E})$

```

1: for  $i$  from 1 to  $M$  do
2:   Create node  $v_i \in \mathcal{V}$  using the centroid  $p_i$  and
   bounding box size  $b_i$  of object point cloud  $P_i$ 
3: end for
4: for  $i$  from 1 to  $M$  do
5:   for  $j$  from  $i + 1$  to  $M$  do
6:      $\text{RelsType}_v \leftarrow \text{VerticalInContact}(v_i, v_j)$ 
7:     Add in-contact vertical relationship triplets
        $(v_i, v_j, e_{i,j})$  with  $\text{RelsType}_v$  to  $\mathcal{G}$ 
8:   end for
9:   if No objects horizontally related to  $v_i$  then
10:    for  $k$  from 1 to  $M$  and  $i \neq k$  do
11:       $\text{RelsType}_v \leftarrow \text{VerticalNonContact}(v_i, v_k)$ 
12:      Add non-contact vertical relationship triplets
         $(v_i, v_k, e_{i,k})$  with  $\text{RelsType}_v$  to  $\mathcal{G}$ 
13:    end for
14:   end if
15: end for
16: for  $v_i \in \mathcal{V}$  do
17:   let  $\{v_{i_1}, v_{i_2}, \dots, v_{i_N}\}$  be the  $N$  different nodes with
   the same in-contact vertical parent node  $v_i$ 
18:   for  $j$  from 1 to  $N$  do
19:      $\text{RelsType}_h \leftarrow \text{Horizontal}(v_i, v_{i_j})$ 
20:     Add horizontal relationship triplets  $(v_i, v_{i_j}, e_{i,i_j})$ 
     with  $\text{RelsType}_h$  to  $\mathcal{G}$ 
21:   end for
22: end for
23: Update  $\mathcal{G} \leftarrow \text{MultiObjects}(\mathcal{G})$ 
24: Update  $\mathcal{G}$  with automatic verification procedure

```

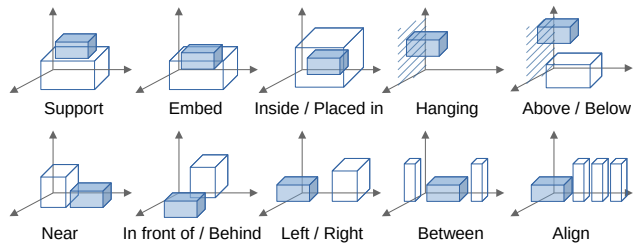


Figure A.1. Overview of the relationships in SCENEVERSE. The target object is colored in blue.

A.3.1 Object Captioning Pipeline

Object captions aim to provide detailed descriptions of an object’s visual and physical properties, facilitating object-level grounding with its distinctive features. The detailed object captioning pipeline is outlined in Alg. 2. Given the multi-view images $\{I_1, I_2, \dots, I_n\}$, we utilize the point cloud P_o of the object o to get the visible points $P_{o,v}^{vis}$ in the images v



Figure A.2. Examples of object captioning. We color the target object in **bold**.

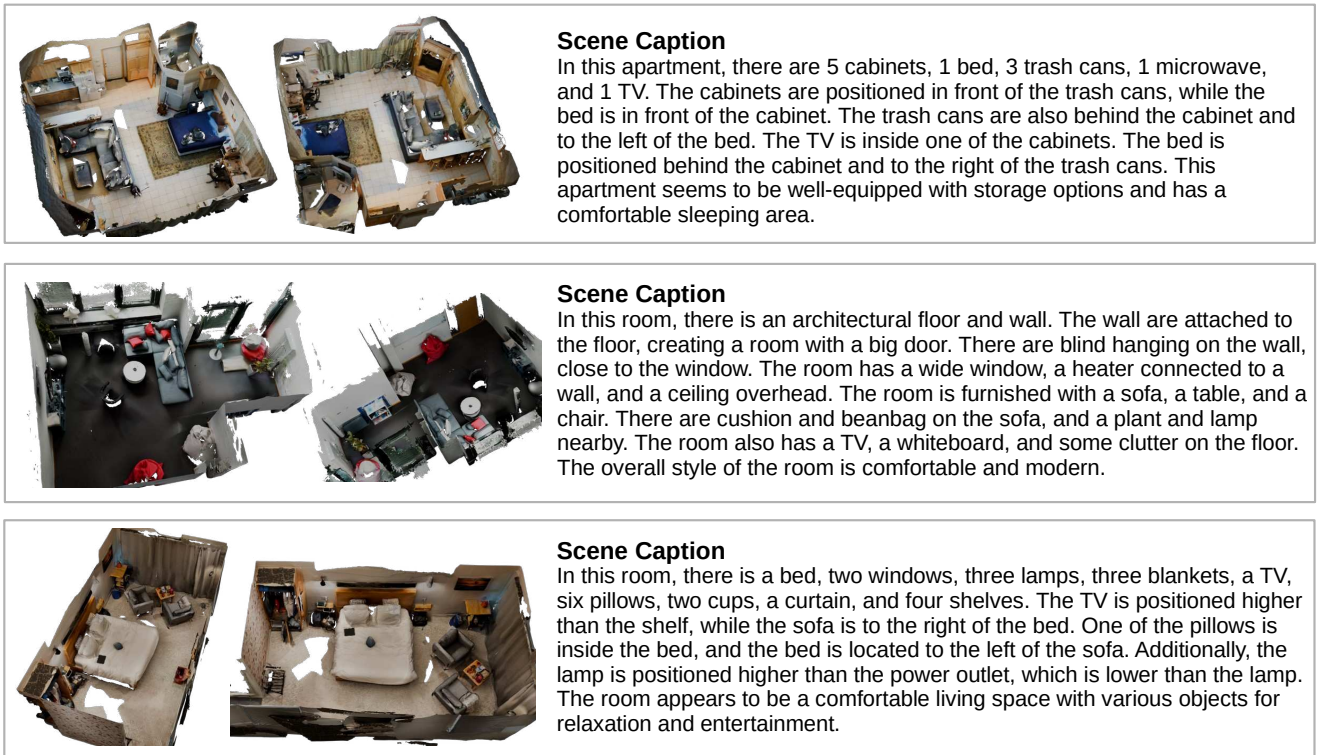


Figure A.3. Examples of scene captioning.

through rendering. The occlusion score $s_{o,v}^{occ}$ is calculated as the ratio between the number of visible points and the object point cloud. The image is then cropped with the rendered bounding box and processed through BLIP2 [48] to generate the initial object caption $C_{o,v}$. For each initial caption, we calculate its CLIP [66] similarity score between the text and the cropped image, denoted by $s_{o,v}^{clip}$. To get a refined object caption, we select the top 10 initial captions with the highest CLIP score and minimal occlusion. The selected sentences are fed into a LLM to obtain a coherent summary of the object captions. In this process, we explicitly instruct the language model to identify and correct the potential errors.

A.3.2 Automatic Language Generation

Template-based We create diverse templates to generate descriptions for each type of relationship. We categorized the templates into three types based on the number of objects involved and their spatial relationships.

- **Pair-wise:** The pair-wise templates are used to describe the positional relationship between the target object and the anchor object in the scene. We design various templates to enrich the templated-based descriptions, spanning active and passive tense, as well as inversion clauses. Typical examples are shown below:

- The **target-object** (is) **spatial-relation** the **anchor-object**.

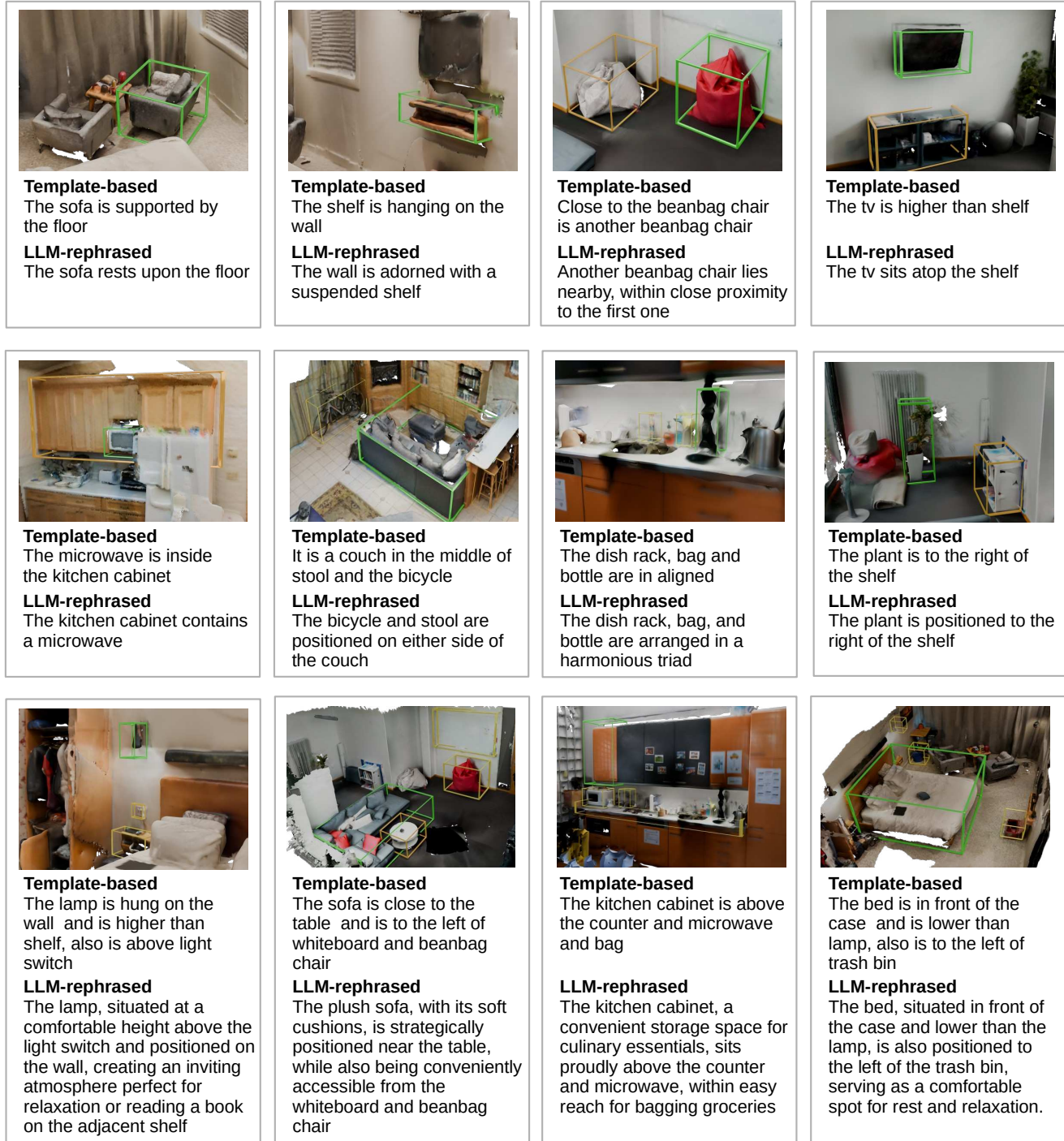


Figure A.4. **Examples of object referral.** Note that the green bounding box indicates the target object and yellow bounding box indicates the anchor object(s).

- It is a **target-object** that (is) **spatial-relation** the **anchor-object**.
- There is a **target-object** that (is) **spatial-relation** the **anchor-object**.
- **Spatial-relation** the **anchor-object** is the **target-object**.
- **Spatial-relation** the **anchor-object**, a **target-object** is placed.
- **Multi-objects:** This is utilized when the target object forms a between or align relationship with multiple anchor objects in the scene. The templates follow the same construction rules as the **Pair-wise** templates.

Algorithm 2: Object Captioning Pipeline

Input : M object point clouds $\{P_1, P_2, \dots, P_m\}$;
 N multiview images $\{I_1, I_2, \dots, I_n\}$
Output: Captions for each object in the scene
 $\{C_1, C_2, \dots, C_m\}$

- 1: **for** $o = 1, 2, \dots, M$ **do**
- 2: **for** $v = 1, 2, \dots, N$ **do**
- 3: Project P_o on I_v to get visible points $P_{o,v}^{vis}$
- 4: Crop I_v with the bounding box of $P_{o,v}^{vis}$ to get $I_{o,v}^{crop}$
- 5: Get the image caption $C_{o,v}$ for $I_{o,v}^{crop}$ using BLIP2 [48]
- 6: Calculate the similarity score $s_{o,v}^{clip}$ between $C_{o,v}$ and $I_{o,v}^{crop}$ with CLIP [66]
- 7: Calculate the occlusion score $s_{o,v}^{occ} = \frac{\#P_{o,v}^{vis}}{\#P_o}$
- 8: **end for**
- 9: Select the top-10 $\{C_{o,v}\}$ with highest $s_{o,v}^{clip} * s_{o,v}^{occ}$
- 10: Summary selected $\{C_{o,v}\}$ with GPT-3.5 to get C_o
- 11: **end for**

- **Star-reference**: To increase complexity in templated-based descriptions, we design “star-reference” to describe the target object and its relationship with 3 randomly selected anchor objects in the scene graph. In particular, we perform cluster analysis on the selected relationship triplets. Based on the diversity of the analysis, different templates will be chosen to generate descriptions. For example, when the relations between 3 anchor objects and the target object is the same, we prefer to use the template like: “The **target-object** (is) **spatial-relation** the **anchor-object-1**, **anchor-object-2** and **anchor-object-3**”. If 2 out of the 3 anchor objects have the same relations with the target object, we would use a template like: “The **target-object** (is) **spatial-relation-1** the **anchor-object-1** and **anchor-object-2**, and (is) **spatial-relation-2** the **anchor-object-3**”.

LLM-rephrasing To increase description diversity we use the GPT-3.5[61] and Llama[75] for description rephrasing. This improves the diversity and naturalness of the template-based descriptions, as is shown in Fig. 2. The detailed prompts are provided in Tab. A.2.

More examples of the scene-language pairs in SCENEVERSE are shown in Fig. A.2, Fig. A.3 and Fig. A.4.

B. Model Details

B.1. Spatial-Attention Transformer

In Sec. 4.2, we leveraged and spatial-attention based transformer architecture to aggregate object-level point cloud features with spatial location information. In this section,

we provide the detailed design of this proposed module.

Formally, given object features $\{f_i^O\}_{i=1}^N$ and their locations $\{l_i\}_{i=1}^N$, we first construct pair-wise spatial relationship feature via:

$$m_{ij} = [d_{ij}, \sin(\theta_h), \cos(\theta_h), \sin(\theta_v), \cos(\theta_v)],$$

where d_{ij} denotes the Euclidean distance between objects and θ_h, θ_v are the horizontal and vertical angles of the line connecting the centers of objects i, j . We then use this pair-wise relationship feature $M = [m_{ij}] \in \mathbb{R}^{N \times N \times 5}$ to modulate the attention weights of the self-attention layer in the transformer when aggregating object features as shown below:

$$\text{Attn}(Q, K, V, M) = \text{softmax} \left(\frac{QK^T}{\sqrt{d_h}} + \log \sigma(M\omega) \right) V,$$

where $\omega \in \mathbb{R}^5$ is a projection layer mapping spatial pair-wise features to the attention scores and σ denotes the sigmoid function. This process could be equivalently interpreted as using the spatial location of objects to adjust the self-attention feature aggregation between objects, making spatially related objects have more attention weights.

B.2. Pre-training Details

For training our model GPS, we conduct a two-stage training approach. As described in Sec. 4.3, we first pre-train the object point cloud encoder with the object-level grounding objective. Next, we freeze the object point cloud encoder during the second pre-training stage for scene-level pre-training that includes model training with scene-level grounding and referral object grounding objectives. This design is inspired by recent works like [21, 98] that demonstrated a well-grounded initialization of object representations is beneficial for 3D scene grounding.

Object-level pre-training To correctly align objects in scenes with their captions, we utilize the ground-truth object bounding boxes provided with the datasets to segment all objects in the scenes. Next, we utilize a PointNet++ [65] encoder to encode and align these object point clouds with object captions provided in SCENEVERSE following Sec. 4.1. For object instances with no object captions synthesized, we follow [66] and construct captions with their semantic class labels like “the point cloud of <CLASS>”. Notably, as our model design sets no constraints on object point cloud encoders, the choice of object encoder mainly depends on the computing resources available.

Scene-level pre-training With pre-trained object feature extractors, we further use both scene captions and object-referring expressions for scene-level pre-training. We use a 4-layer BERT encoder for encoding both scene captions and object referrals. As discussed in Sec. 4.2, we apply a 4-layer spatial transformer to encode object features with their locations. For scene-level grounding, we adopt a max-pooling

Table A.2. Prompts used in SCENEVERSE.

Description type	Prompt
Object caption	<p>Summarize caption below. The summary should be a description of the target-object. Focus on the target-object's attribute, like color, shape and material, <i>etc.</i> Identify and correct the potential errors.</p> <p>caption: <i>A bed in a hotel room. A white comforter on a bed. A bed with a striped comforter..</i></p> <p>target-object: <i>Bed</i></p>
Object referral	<p>Rewrite the following caption using one random sentence structure. You should give me only one rewritten sentence without explanation.</p> <p>caption: <i>The bed is between desk and nightstand.</i></p> <hr/> <p>Rewrite the following caption. You should give me only one rewritten sentence about target-object without explanation. Make sure target-object is the subject of the sentence, not anchor-object(s). If the sentence is in full inversion, keep the inversion.</p> <p>caption: <i>The armchair is next to the sofa.</i></p> <p>target-object: <i>Armchair</i></p> <p>anchor-object(s): <i>Sofa</i></p> <hr/> <p>Rewrite the following caption using one random sentence structure. You need to focus on the location and relations of the target-object that appears in the sentence. If multiple target-object appear in the sentence, you need to focus on the first target-object that appears. You can also add the target-object's function and comfort level based on the sentence, e.g., how the objects can be used by humans and human activities in the scene. You should give me only one rewritten sentence without explanation.</p> <p>caption: <i>Far from the bowl and peppershaker, the vase is to the left, it is also on the top of countertop.</i></p> <p>target-object: <i>Vase</i></p>
Scene captioning	<p>Your task is to provide a summary for a scene from a given scene graph. The scene contains some objects, which compose a scene graph in json format.</p> <p>There are 3 types of descriptions in scene graph: "scene type" denotes the type of the scene. "objects count" then listed the objects in the scene and their quantity, it should be noted that the actual objects in the room may be more than listed. "objects relations" describe the spatial relations with objects.</p> <p>Also describe the scene concerning commonsense, e.g., how the objects can be used by human and human activity in the scene. The description should conform to the given scene graph. The spatial relations between objects can only be inferred from the "objects relations" in scene graph. Don't describe each object in the scene, pick some objects of the scene for summary. Don't describe each relations in the scene, pick some relations of the scene for summary. You can also summarize the room's function, style, and comfort level based on the arrangement and count of objects within the room. The summary should be about the object types, object attributes, relative positions between objects. Your summary must not exceed 80 words. You must write using one random sentence structure.</p> <p>scene graph: { 'scene_type': 'Bedroom', 'object_count': {'nightstand':2, ...}, 'relation': {'nightstand', 'on', 'floor'}, {'backback', 'in front of', bed}, ... }</p>

layer to aggregate features from the spatial transformer and align with the [CLS] feature of the scene caption. For referral-object-level grounding, we further pass the obtained object features as well as the referral language features into a 4-layer self-attention transformer and use the grounding objective described in Sec. 4.3 to match the referred object's feature and the [CLS] feature of the referring expression.

Training For object-level pre-training, we utilize an AdamW optimizer with a learning rate of 1×10^{-2} for 1500 epochs and no warm-up periods. During training, we use a batch size of 512 and leverage a cosine annealing scheme for learning rate scheduling with a minimum learning rate of 1×10^{-3} . For scene-level pre-training, we use an AdamW

optimizer with a learning rate of 1×10^{-5} for the language encoder, a learning rate of 1×10^{-4} for the spatial transformer, a learning rate of 1×10^{-4} for the self-attention transformer, and a learning rate of 5×10^{-4} for all remaining learnable parameters (*e.g.*, projections). For all experiments, we train the model for 150 epochs with a warm-up period of 500 and also a cosine annealing scheme for learning rate with a minimum learning rate ratio of 0.1. All pre-training experiments are run on 8 NVIDIA-A100 GPUs with the longest pre-training on SCENEVERSE taking about 2 days.

C. Experimental Details

In this section, we provide details on experimental settings, model implementation, and additional results.

C.1. 3D Visual Grounding

Setting For all datasets, we evaluate all models with only the training sets provided. Following previous works [98], we report model performance on the validation set of all datasets in Tab. 2. Notably, we used an off-the-shelf Mask3D segmentation model for generating object proposals with no optimization.

Implementation As briefly mentioned in Sec. 5.1, we mainly considered three model settings in 3D visual grounding experiments, namely *scratch*, *pre-train*, and *fine-tuned*. For the *pre-train* setting, we follow the same setting mentioned in Appendix B.2. In the *scratch* and *fine-tuned* settings, to fairly compare with other dataset-specific fine-tuned models, we add an additional 2-layer MLP over the object features from the referral grounding self-attention transformer. During training, we fine-tune this grounding head together with all model weights for 100 epochs with a learning rate of 1×10^{-4} for the added projection layer and set all other settings the same as the implementation described in Appendix B.2.

C.2. Zero-shot Transfer

Setting In the zero-shot experiments, we first construct the held-out test set by aggregating scene-text pairs in SCENEVERSE from scenes in ScanNet and MultiScan. Specifically, we use the validation set of ScanRefer, Nr3D, and Sr3D. For scene-text pairs in the SCENEVERSE-val, we construct the test set by randomly sampling $\frac{1}{5}$ of human-annotated object referrals in the MultiScan dataset. This results in a test set with around 1.7K object referrals randomly drawn from 8.5k human-annotated object referrals in the MultiScan dataset. In the *zero-shot* settings, we use all scene-text pairs from datasets in SCENEVERSE except for ScanNet and MultiScan. This includes both human-annotated and generated texts in ARKitScenes, 3RScan, and HM3D. This setting serves to test models’ generalization capability in grounding objects with both unseen scenes and unseen texts. In the *zero-shot text* setting, we add generated scene-text pairs in ScanNet and MultiScan into the data used in the *zero-shot* setting, thereby making the held-out test containing mainly unseen object referrals.

Implementation In the zero-shot experiments, we mainly considered three model settings *scratch*, *zero-shot*, and *zero-shot text*. For the *zero-shot* setting, we pre-train the model following Appendix B.2 without additional grounding heads considering there is no additional training data available in the zero-shot transfer setting. In the *scratch* and *zero-shot text* setting, we follow the model implementation

Table A.3. **Semantic segmentation results on ScanNet validation set.** † denotes model trained with surface normals as an additional input. S3D indicates models initialized with the original SWIN3D model weights pre-trained on Structured3D provided by Yang *et al.* [85].

Methods	Init.	SCENEVERSE Pre.	mIoU	mAcc
SWIN3D _n -S†	✗	✗	75.2	-
SWIN3D _n -S†	S3D	✗	75.6	-
SWIN3D-S	✗	✗	63.2	72.8
SWIN3D-S	S3D	✗	64.1	75.1
SWIN3D-S (<i>pre-train</i>)	✗	✓	67.7	78.0
SWIN3D-S (<i>pre-train</i>)	S3D	✓	69.5	80.1
SWIN3D-S (<i>fine-tuned</i>)	S3D	✓	70.6	80.2

described in Appendix C.1 and add an additional 2-layer MLP over the object features from the self-attention transformer. We follow the same fine-tuning setting described in Appendix C.1.

D. Additional Results

In this section, we provide additional experimental results. Specifically, we leverage our collected SCENEVERSE as the pre-training data source for a traditional 3D semantic segmentation task. Next, we provide ablative analyses of our model design.

D.1. Semantic Segmentation

Setting To test if the scaling effect of SCENEVERSE is universally beneficial for 3D understanding tasks, we use 3D semantic segmentation as a signature task to illustrate the effectiveness of SCENEVERSE. Notably, a recent work that introduced the Swin3D model [85] has identified the importance of pre-training for 3D semantic segmentation [85]. Following the same setting, we test if the proposed SWIN3D model could be further improved by substituting the pre-training data to SCENEVERSE. Specifically, we test models’ performance on the ScanNet semantic segmentation task with 20 semantic categories and report the mean IoU and mean Acc on the validation set of ScanNet. As the original implementation of SWIN3D pre-training requires surface normals as additional inputs, we reimplement the model and pre-train all models with only point coordinates and colors.

Comparison As shown in Tab. A.3, we observe a significant model performance improvement ($\sim 6\%$) by training SWIN3D-S model on our SCENEVERSE dataset. Comparing our pre-training set to Structured 3D, we also observe consistent model performance improvement, showcasing the benefit of scaling-effect in SCENEVERSE. Moreover, we fine-tune the model on ScanNet after pre-training on SCENEVERSE. This process further brings improvement in model performance on semantic segmentation. We believe these results serve as strong pieces of evidence validating the effectiveness of data scaling in SCENEVERSE and also

Table A.4. **Model ablation of our model on SCENEVERSE-val.**

Obj-lvl	MLM	Scene-lvl	Overall	Easy	Hard
✗	✗	✗	64.8	75.4	48.7
✓	✗	✗	65.2	77.1	47.4
✓	✓	✗	62.4	73.4	45.8
✓	✓	✓	66.9	77.8	50.3

its potential benefit for all 3D tasks in addition to 3D visual grounding.

D.1.1 Model Ablation

In this section, we provide ablative analyses of our multi-level contrastive alignment design. We mainly consider removing objectives in our model as ablations. We choose the referral-object-level alignment objective as the default setting and consider removing: (i) object-level alignment objective, (ii) masked language modeling objective, and (iii) scene-level alignment objective. For removing the object-level alignment objective, we remove the first stage pre-training of the object point cloud encoder and jointly learn this module within the referral-object-level alignment. As shown in Tab. A.4, we test different model settings on the SCENEVERSE-val without additional fine-tuning. First, we show that the scene-level alignment objective is crucial for referral object grounding in SCENEVERSE-val with the $\sim 5\%$ performance drop. Similar observations could be made for the model trained without object-level alignment ($\sim 2\%$ drop) and masked language modeling objective ($\sim 1.5\%$ drop). We believe these results affirm the effectiveness of our overall model design.